GEOLOGICA CARPATHICA, JUNE 2011, 62, 3, 279–295 doi: 10.2478/v10096-011-0022-y

Neotectonics, drainage pattern and geomorphology of the orogen-parallel Upper Enns Valley (Eastern Alps)

MELANIE KEIL[1] and FRANZ NEUBAUER[2]

Division of General Geology and Geodynamics, Department Geography and Geology, University of Salzburg, Hellbrunner Straße 34, A-5020 Salzburg, Austria; Melanie.Keil2@sbg.ac.at; Franz.Neubauer@sbg.ac.at

(Manuscript received March 3, 2010; accepted in revised form October 13, 2010)

Abstract: The geomorphology and neotectonics of the Upper Enns Valley (Austria) in the Eastern Alps reveal the formation of a fault-controlled orogen-parallel valley. In the study area, the Eastern Alps have been under surface uplift since Early Miocene times. Quaternary processes such as uplift and cyclic glaciations likely interfere with neotectonic activity as the Upper Enns Valley follows the Salzach-Enns-Mariazell-Puchberg (SEMP) fault. The geomorphologically different landscapes comprise three main tectonic units: (1) the Austroalpine crystalline basement exposed in the Niedere Tauern, (2) the Austroalpine Paleozoic units (Greywacke Zone) and (3) the Dachstein Plateau dominated by Triassic carbonate successions. The Upper Pleistocene Ramsau Conglomerate overlying the Greywacke Zone on the northern slope of the Upper Enns Valley is a crucial element to reconstruct the evolution of the valley. A new ^{14}C date (uncalibrated) indicates an age older than 53,300 years, outside of the analytical limit of the methods. Provenance analysis of the Ramsau Conglomerate shows the Niedere Tauern as a source region and consequently a post-early Late Pleistocene dissection of the landscape by the Upper Enns Valley. Paleosurfaces at elevations of about 1100 m on the northern and southern slopes of the Upper Enns Valley allow us to estimate surface uplift/incision of about 2.5 mm/yr. Regularly oriented outcrop-scale faults and joints of the Ramsau Conglomerate document Pleistocene to Holocene tectonic deformation, which is consistent with ongoing seismicity. Paleostress tensors deduced from slickensides and striae of pre-Cenozoic basement rocks indicate two stages of Late Cretaceous to Paleogene deformation independent of the SEMP fault; the Oligocene–Neogene evolution comprises NW–SE strike-slip compression followed by E–W compression and Late Pleistocene ca. E–W extension, the latter recorded in the Ramsau Conglomerate.

Key words: Quaternary, Eastern Alps, seismicity, tectonic deformation, paleostress analysis, provenance analysis, Ramsau Conglomerate Formation.

Introduction

The study focuses upon the upper section of the Enns River, which is one of the largest tributaries to the Danube in Austria and emphasizes the dominating forces that contributed to the present-day diversity of morphology of the Upper Enns Valley.

The dynamic evolution of a fault-controlled valley and its drainage system cannot be seen as an isolated process but in the context of the landscape involved. Surface uplift of mountains, rivers and drainage patterns, faults, erosion and sedimentation as well as climatic impacts are reflected by the landscape (Kuhlemann et al. 2001a). As a result of the collision of the European and Adriatic plates, the morphogenetic evolution of the Eastern Alps started in the Oligocene (from ca. 30 Ma onwards; Frisch et al. 2000a). Approximately N–S directed plate convergence caused thrusting and crustal thickening during continental collision (Ratschbacher et al. 1989, 1991; Peresson & Decker 1997a,b; Neubauer et al. 2000; TRANSALP Working Group 2002). Crustal thickening and isostatic uplift formed the first coherent relief (Hejl 1997). The tectonic evolution was driven by shortening of the orogenic wedge and by onset of the eastward oriented lateral extrusion of the Central Eastern Alps. An important feature of eastern sectors of the Northern Calcareous Alps and central sectors of the Eastern Alps is the Miocene Salzach-Enns-Mariazell-Puchberg (SEMP) fault striking WSW–ENE over 400 km from the northern Tauern Window in the west to the Vienna Basin in the east (e.g. Ratschbacher et al. 1991; Linzer et al. 1997). The SEMP-fault represents the northern margin of the principal eastward extruding block. During Early and Middle Miocene times, the Adriatic plate continued to move towards the stable European lithosphere (Ratschbacher et al. 1989, 1991). The southern sectors of the Eastern Alps experienced crustal shortening, and, in the northern sectors of the Eastern Alps, numerous, mostly orogen-parallel sinistral strike-slip fault-systems were the consequence of indentation. N–S shortening changed from thrusting and crustal thickening to lateral extrusion and orogen-parallel extension (Ratschbacher et al. 1989, 1991; Peresson & Decker 1997a,b; Frisch et al. 1998, 2000b; Sachsenhofer 2001), and affected and formed the topography of the Eastern Alps in Early to Middle Miocene times (Fig. 1a). Strong Neogene strike-slip tectonics were responsible for not only the eastward extrusion of the Austroalpine upper crust but also for the development of the west-east trending fault-controlled Paleo-Enns Valley with tributary rivers, the Paleo-Mur-Mürz (Dunkl et al. 2005) and locally fault-controlled basins. Investigations in the westernmost Wagrain sedimentary basin between Altenmarkt and Wagrain (Fig. 1b) demonstrate that the development of the basin is concurrent with the formation of the SEMP and Mandling faults in Early Miocene times (Wang & Neubauer 1998; Neubauer 2007).

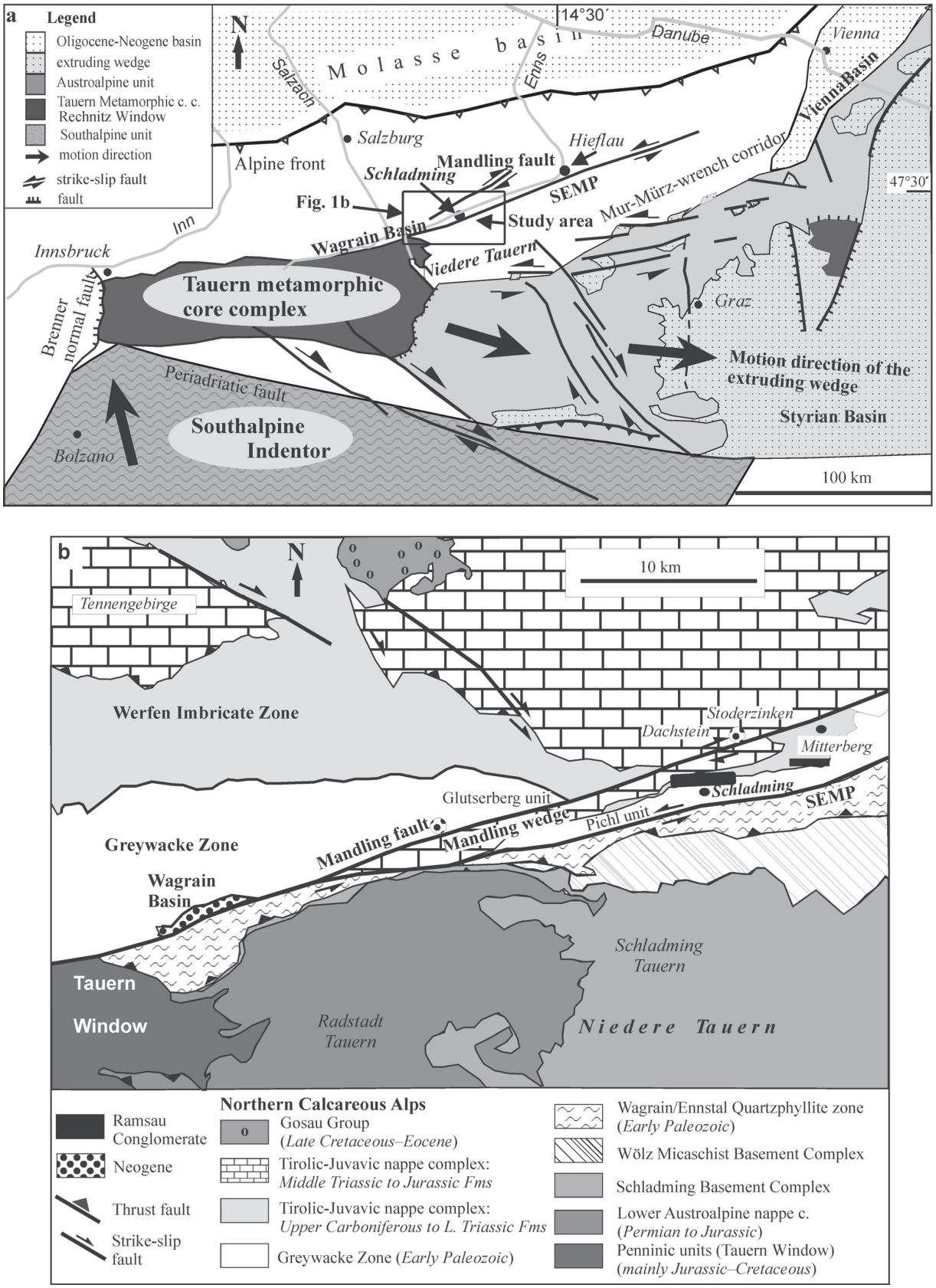

Fig. 1. a — Simplified tectonic map of the Eastern Alps showing N–S shortening and lateral extrusion (modified after Keil & Neubauer 2009; credit to Österreichische Geologische Gesellschaft). **b**— Simplified geological map of the Upper Enns Valley region showing major structural units.

Some major extrusion-related fault zones are recognized to be still active, among others, the SEMP fault (Reinecker & Lenhardt 1999; Lenhardt et al. 2007); shallow low-magnitude earthquakes have been reported from the study area (M 0.7–4.1).

We document, for the first time, deformation structures in a Pleistocene conglomerate and use geomorphological features to deduce steps of surface uplift of the region. We also present a new ^{14}C-age of lignite from the Ramsau Conglomerate documenting an older age of this formation than previously suggested.

Materials and methods

Basic materials are the topographic maps ÖK 25V, sheet 127 Schladming and sheet 128, Gröbming, Geologische Karte der Republik Österreich, 1:50,000, sheet 127 Schladming (Mandl & Matura 1995), and digital elevation models (DEM). Fieldwork focused on the Ramsau Conglomerate, the tributaries of the Enns River and the Schladming Basement Complex and comprised geomorphological and sedimentological investigations. A provenance analysis and structural analyses of the Ramsau Conglomerate were carried out in detail. The approach of the provenance analysis of conglomerates followed Ritts et al. (2004) and Yue et al. (2003). Slickenside and striation data were collected along the tributaries of the Enns River and at the bottom of the Schladming Basement Complex. Paleostress orientation patterns of faults and slickensides were evaluated by using the Tectonics FP computer programme (Ortner et al. 2002).

Geological and geomorphological setting

The ENE-trending sinistral SEMP fault (Ratschbacher et al. 1991; Wang & Neubauer 1998) is supposed to run along the Upper Enns Valley in the study area. The fault itself is largely hidden by the Holocene valley fill (alluvial deposits) and is likely located along the southern margin of the valley. The Upper Enns Valley separates the crystalline basement of the Schladming Tauern as part of the Niedere Tauern in the south from the Greywacke Zone and the Northern Calcareous Alps with the Dachstein plateau in the north (Fig. 2). In addition, the ENE-trending dextral Mandling fault transects the Greywacke Zone, and the Mandling wedge, composed of Mesozoic rocks of the Northern Calcareous Alps, is exposed to its south. The Mandling wedge is interpreted as representing a strike-slip duplex of the Northern Calcareous Alps.

The southern and the northern slopes of the Upper Enns Valley differ significantly in geomorphology and geology. Three geomorphologically different types of landscapes are characteristic for the main tectonic units, namely the Austroalpine crystalline basement with gneisses, granites and micaschists represented by the rugged relief in the Niedere Tauern, the Austroalpine Paleozoic unit (Greywacke Zone)

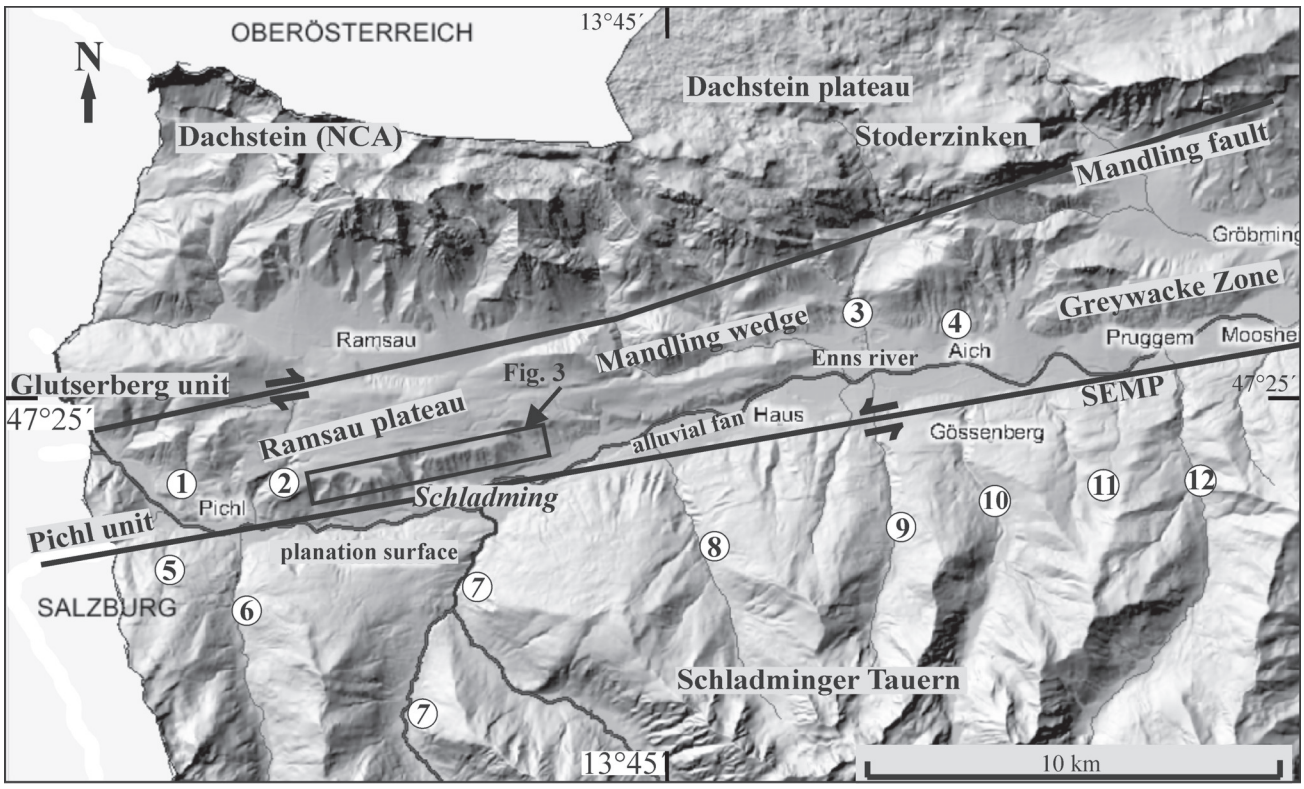

Fig. 2. Digital elevation model of the study area indicating the geological and geomorphological setting. Numbers refer to locations of main tributaries to the Enns River shown in Fig. 4: **1** — Grubbach, **2** — Grießenbach, **3** — Gradenbach, **4** — Aichbergbach, **5** — Eisbachgraben, **6** — Preuneggbach, **7** — Talbach/Obertalbach, **8** — Dürrenbach, **9** — Gumpenbach, **10** — Seewigtalbach, **11** — Auerbergbach, **12** — Sattentalbach.

with lithologies of high erosivity and the Permomesozoic cover rocks dominated by Triassic carbonate sequences with steep rock faces and the Oligocene/Early Miocene Dachstein plateau on top.

Pronounced geomorphological differences can be observed between the northern and southern valley flanks. The Ramsau plateau (ca. 1100 m a.s.l.) is located ca. 340–360 m above the present-day valley bottom; its southern boundary displays sharp-edged scars (Fig. 2). Fine-grained sediments promote water outlet, resulting in deeply carved channels. Alluvial fans on the north side of the valley display scars ca. 20 m above the present-day valley bottom.

The southern tributary valleys form larger alluvial fans than those from the northern side and significant canyons, epigenetic gorges and distinct knick zones. The valleys are narrow; the valley slopes are steep or subvertical. Mass movements and landslides, which developed on weak phyllite lithologies of the Ennstal Quartzphyllite zone, have shaped the slopes facing the valley.

Stratigraphic units

The Schladming Basement Complex (part of the Niedere Tauern) is exposed on the southern side of the Upper Enns Valley (Fig. 1b). This complex consists of a polymetamorphic, Variscan and Alpidic basement with medium- to low-grade para- and orthometamorphic rocks (Mandl & Matura 1987). Para- and orthogneiss, migmatite-gneiss, quartz-phyllite, sericite-quartzite, greenschist, and amphibolite are the most frequently occurring rocks in the Schladming Basement Complex. The westernmost part belongs to the Lower Austroalpine units of the Radstadt Tauern with the Permian Alpine Verrucano-type Quartzphyllite Group and the Lower Triassic Lantschfeld Quartzite at its stratigraphic base (Mandl & Matura 1987). To the south of the Upper Enns Valley, the Schladming Basement Complex is overlain by the Wölz Micaschist unit and the Ennstal Quartzphyllite or its western extension, the Wagrain Quartzphyllite. The Schladming Basement Complex exhibits a young morphology with steep slopes, and reaches elevations up to 2800 m a.s.l. (Reinecker 2000; Frisch et al. 2000a).

North of the Upper Enns Valley, in the wider Schladming area, the Pichl unit represents the southern, structural lower element of the Greywacke Zone and the Glutserberg unit the higher one, exposed farther north (Fig. 2). These are separated by the Mandling wedge. The Pichl and Glutserberg units comprise phyllites rich in quartz veins and lenses, greenschist, grey metasandstone, and rare calcite and dolomite marble intercalations. The Mandling wedge comprises rare lenses of Lower Triassic Werfen Quartzite cut at the base by faults, mainly Middle Triassic Gutenstein Dolomite and Upper Triassic Dachstein Limestone (Matura 1987). Greywacke Zone and Mandling wedge are at relatively low elevations reaching maximum altitudes of 1760 m.

The Glutserberg unit is overlain by the Permian to Upper Jurassic succession of the Dachstein block, which is part of the Northern Calcareous Alps. The succession includes Permian to Lower Triassic siliciclastic formations (Alpine Verrucano and Werfen Formations). These lithologies display a similar geomorphological expression to the Greywacke Zone. A thick Middle to Upper Triassic dolomite and limestone sequence including the Upper Triassic Dachstein Limestone forms impressive, steep rock faces. Jurassic formations are rare. The Dachstein Limestone forms a plateau at elevations of ca. 2200–2400 m and peaks up to 3000 m a.s.l. Miocene clastic rocks, the so-called Augenstein Formation comprising mainly well rounded vein-derived quartz pebbles have been found on the plateau and in karst holes (Frisch et al. 2002; Seebacher 2006, e.g. Dachstein south face at 1770 m a.s.l.). This proves that the Dachstein plateau is a karstified, Lower Miocene paleosurface covered by fluvial deposits, now uplifted to its present elevation (Frisch et al. 2001).

The Upper Pleistocene Ramsau Conglomerate overlies the Pichl unit of the Greywacke Zone and forms much of the landscape of the northern slope of the Upper Enns Valley between Pichl and Weißenbach/Haus (Fig. 3). Here, we introduce the informal term Ramsau Conglomerate Formation for this section. The base of the Ramsau Conglomerate Formation is at an elevation of ca. 820 m in the west (Pichl) and ca. 780 m in the

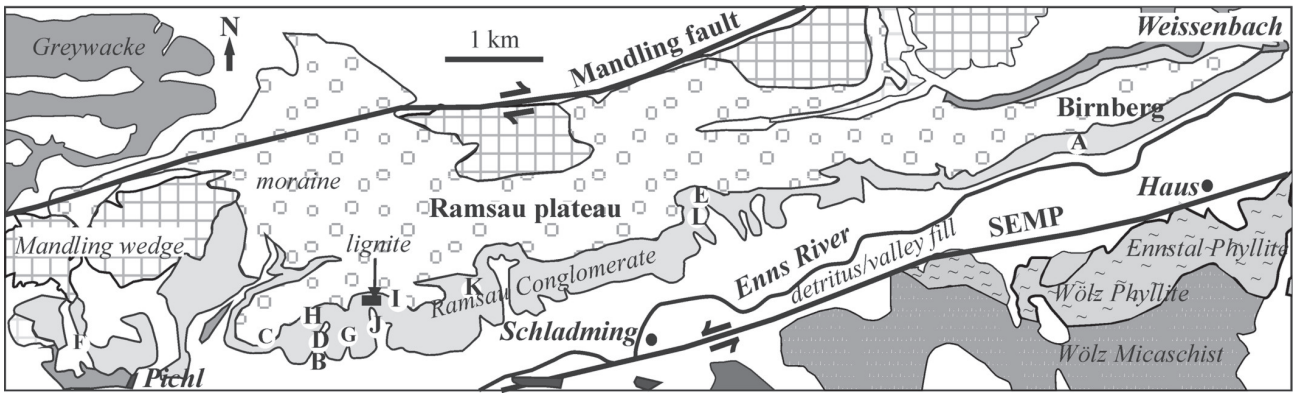

Fig. 3. Simplified geological map of the study area (with main emphasis on the Pleistocene Ramsau Conglomerate Formation) between N 47°23.652/E 013°36.506 and N 47°24.806/E 013°44.917. The E–W distance is about 12 km (modified after Mandl & Matura 1995). **A–K** — outcrops for provenance analysis, **L** — location of Fig. 12, **SEMP** — Salzach-Enns-Mariazell-Puchberg fault.

east (Birnberg road near Oberhaus railway station), and its top forms an impressive planation surface, the Ramsau plateau at an elevation of ca. 1100 m a.s.l. The conglomerate comprises mainly a polymict conglomerate dominated by metamorphic pebbles, rare sandstones and a widespread subhorizontal coal/lignite seam at an elevation of ca. 965 m (Fig. 3). The coal appears dark brown, shrunk and shows the megascopic characteristics of lignite (Weber & Weiss 1983; Sachsenhofer 1988). It was subject to underground exploitation until 1947 (Weber & Weiss 1983; Weiss 2007). The uncalibrated ^{14}C age is 31 ± 1.2 ka (van Husen 1987). The age of this lignite seam is still uncertain in spite of spore/pollen analyses (Draxler 1977; Draxler & van Husen 1978). The ^{14}C age is at the limit of the method. Earlier opinions argue for an age of deposition in the Riss/Würm Interglacial (e.g. Sachsenhofer 1988). The Ramsau Conglomerate Formation is covered by Upper Pleistocene moraines and Holocene rivulets are incised into it.

Results

Drainage pattern

Though the fluvial channel of the Enns River represents only a small proportion of the landscape in the study area, together with its tributaries from N and S, it may be the key to explaining external and tectonic geological processes, which resulted in formation of the present-day morphology. All tributaries are oriented aproximately perpendicular to the Upper Enns Valley. The Enns River flows near the southern valley side, except where large alluvial fans coming from the southern tributaries force a distal flow. The longitudinal valley of the Enns River has one characteristic feature, namely an asymmetric drainage pattern of tributary rivers (Zötl 1960; Keil & Neubauer 2009). Less than 15 percent of the drainage area is located north of the Enns Valley. Tectonically undisturbed rivers have a concave longitudinal profile, steeper near the source, shallow at lower reaches of the rivers. The gradients of the tributaries to the Enns River are not smooth at all; steep reaches change with sections of gentle gradients with pronounced knick points in between (Fig. 4). The profiles of twelve tributaries show clear variations of the river gradients, sometimes within rather short distances. To calculate the river gradients we used the method of Burbank & Anderson (2001): elevation change/length of the reach. The northern tributaries of the Enns River represent short valleys (2–5.5 km) compared to those from the south, which are up to 15.5 km in length. Significant for the majority of the tributaries from the north is the low gradient over a long distance before their confluence with the Enns River (Fig. 4a).

The tributaries from the south caused accumulation of comparably large alluvial fans on which most major villages are located (Fig. 2). Each tributary shows profiles with several knick points followed by steep sections. These steep reaches often include waterfalls (e.g. Gradenbach, Seewigtalbach) and canyons (Talbach, Dürrenbach) in crystalline bed rocks, whereas the infill of flat parts includes characteristic lake sediments and high moors.

Flat reaches over long distances are an outstanding feature of the rivers, the sources of which lie at or above 1700 m, for example, the Preuneggbach (length of flat reach 6400 m), Talbach/Obertalbach (length of flat reach 4000 m), Sattentalbach (length of flat reach 7600 m). The flat reaches are located at elevations between 1000 m and 1100 m (river nos. 6, 7, 10, 11 in Figure 4b) and between 800 m and 900 m (river nos. 6, 7, 10 in Figure 4b). These flat reaches are used to analyse any coincidences between the northern and the southern side of the valley and to reconstruct a possible Pleistocene valley bottom (Fig. 5).

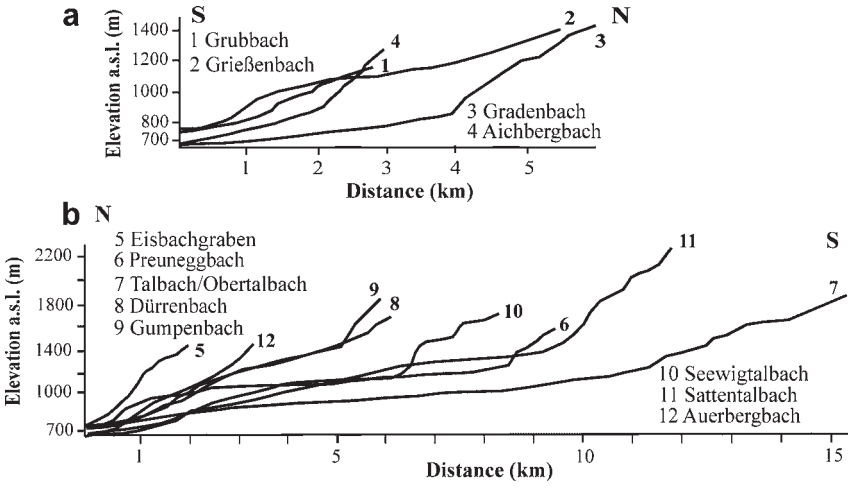

Fig. 4. Longitudinal profiles: **a** — Enns River, tributaries from north, **b** — Enns River, tributaries from south. For locations, see Fig. 2.

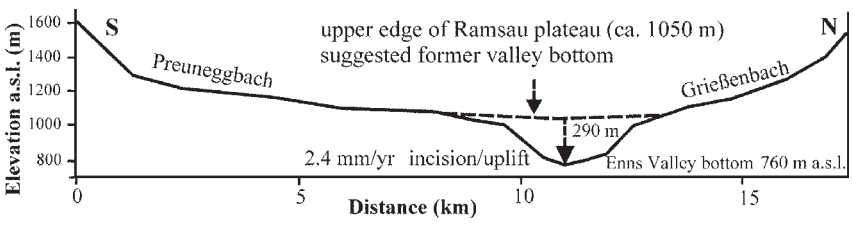

Fig. 5. Longitudinal valley profile Preuneggbach–Grießenbach; these brooks are tributaries from opposite sides of the Upper Enns Valley.

Ramsau Conglomerate Formation: provenance analysis

Descriptions dealing with the conglomerate north of the Upper Enns Valley are rare (Spaun 1964; van Husen 1981, 1987). Today, the stratigraphic sequences of the Ramsau Conglomerate Formation are well exposed from 760 m to ca. 1100 m a.s.l. north of Schladming. The same lithostratigraphic succession

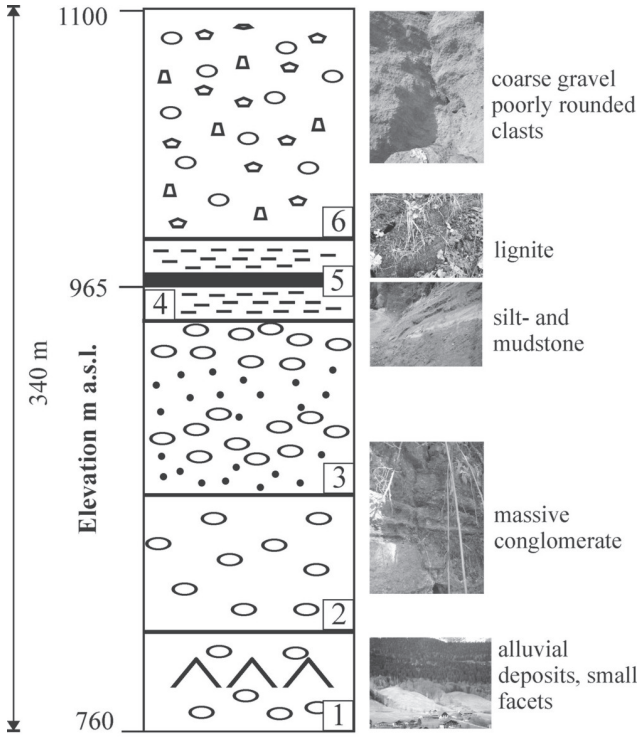

Fig. 6. Stratigraphic sequences of the Ramsau Conglomerate Formation (^^ facets); numbers 1–6 relate to description in the text.

has been observed on the southern slope of Mitterberg, about 10 km farther east (Fig. 1b).

The bedding of the whole section is subhorizontal and the entire section is about 340 m thick (Fig. 6).

The section comprises from base to top: (1) Thick-bedded coarse-grained (2–5 cm) massive conglomerates (ca. 10 m in height) representing deposits of alluvial fans, which are now dissected by small facets; (2) a sharp edge forms the boundary to massive conglomerates, — ca. 20 m in height — with easily accessible outcrops of the Ramsau Conglomerate Formation; (3) above, conglomerates with mostly well-rounded clasts intersected by meter-scaled sandstone layers grade at an elevation of 900 m, into (4) a succession of siltstone and mudstone containing (5) a lignite seam at an elevation of 965 m. Above, (6) a coarse-grained, polymict conglomerate is arranged in 10 m thick beds, the uppermost layers are poorly sorted. A ground moraine covers the Ramsau Conglomerate Formation.

We interpret the conglomerate beds as alluvial fans, according to criteria summarized in Schäfer (2005). On the whole, the lower part of the succession represents a fining upward cycle up to the lignite level. The middle stratigraphic levels with mudstone and lignite are interpreted as lake sediments, already proposed by van Husen (1981) and Draxler (1977). A coarsening upward cycle represents the higher stratigraphic level.

The clast compositions of eleven stations between 768 and 1081 m a.s.l. were determined by counting approximately 100 clasts per exposure on regularly spaced grids, ca. 20×20 cm. Only clasts with a minimum grain size of 1 cm were counted because of easy identification. Results are shown in Figure 7. Clasts originate from: (1) AA crystalline basement (Ennstal Quartzphyllite, paragneiss, orthogneiss, amphibolite, vein quartz); (2) AA metamorphic cover (green quartzite, green quartzitic phyllite, light quartzite, calcitic marble); (3) GWZ (Alpine Verrucano-type quartz-phyllite, vein-derived quartz pebbles, dark quartzite, green quartzite, phyllite, Ennstal Quartzphyllite); (4) NCA (Hallstatt-type limestones, Gutenstein Limestone, red calcitic sandstone as well as dark and light-coloured sandstone from the Werfen Formation at the base of the Northern Calcareous Alps. Hallstatt type limestones are abundant in the NW of the study area, e.g. Scheidleder et al. (2001). There are three groups of clasts: (1) clasts, formed within greenschist-facies metamorphic conditions, (2) clasts of a higher metamorphic grade like amphibolite, para- and orthogneiss as well as marble and quartz-bearing marble (derived from the Schladming and Wölz Basement Complex), and (3) limestones and sandstones derived from the Northern Calcareous Alps.

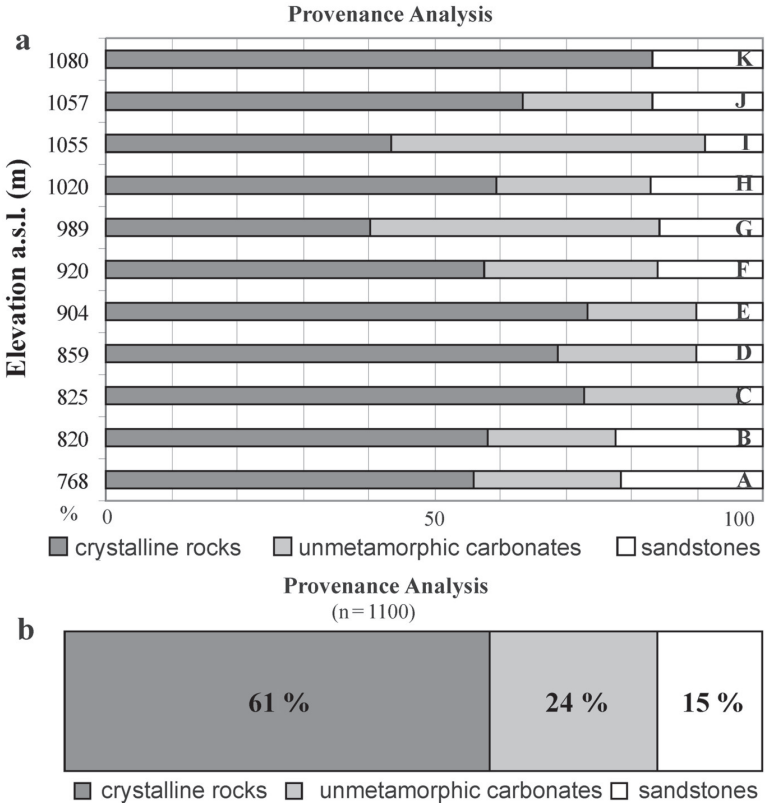

Fig. 7. a — Provenance analysis of the Ramsau Conglomerate Formation at different elevations; A–K refer to sites in Fig. 3; **b** — summarized result of the provenance analysis.

^{14}C dating of lignite

To assess the previously published age of the lignite from the Ramsau Conglomerate Formation (Draxler & van Husen 1978) we collected a new lignite sample at 965 m a.s.l. by excavation. The sample coordinates are N 47°23′49.403″, E 13°38′42.433″. The ^{14}C analysis was performed by accelerator mass spectrometry at the VERA facility of the University of Vienna (VERA-5152, sample Ramsau 1). The analytical data are given in Table 1 (Appendix). The ^{14}C abundance is below the detection limit representing a ^{14}C-age older than 53,300 years.

Glacial overdeepening of the Upper Enns Valley

The Upper Enns Valley is filled with Holocene gravels, and the overdeepening of the valley is explained by glacial carving (Spaun 1964; van Husen 1987; Becker 1987; Reitner & van Husen 2007).

The ablation area of the Würm glaciations formed large overdeepened parts of the valley (van Husen 2000). Drillings and results of geophysical surveys (Becker 1981, 1987) give improved information about sediment thickness and the position of the underlying bedrock in the Upper Enns Valley (Fig. 8). It shows that glacial overdeepening between Mandling and Wörschach is of greater extent than originally assumed (Becker 1981, 1987). At Mandling, the valley fill is about 150 m, the bedrock lies at 650 m a.s.l. The Quaternary fill of 120–130 m suggests the bedrock at Schladming at 595 m a.s.l. which results in a rather constant river gradient of about 0.5 % (Frisch et al. 2000). Recent seismic profiling in the eastern Enns Valley (between Liezen and Weng) shows ca. 480 m of Quaternary sediments (Schmid et al. 2005).

Paleostress in the basement

Geological considerations and large-scale offsets indicate a sinistral transtensional motion with the northern block moving down along the SEMP (Genser & Neubauer 1989; Ratschbacher et al. 1991; Wang & Neubauer 1998; Keil & Neubauer 2009). Detailed fault-slip data and their paleostress assessment from the SEMP fault were mainly published from a segment north of the Tauern Window (Wang & Neubauer 1998) and from the easternmost sectors of the Northern Calcareous Alps (Nemes et al. 1995). From the Upper Enns Valley, no data were published and our aim is to fill this gap.

A list of investigated stations together with geographical situations and lithological descriptions is given in Table 2 (Appendix). The sense of slip was deduced from offset markers, Riedel shears, the surface morphology of slickensides and quartz fibers. The raw data contain partly fault-slip sets with incompatible slip-sense; the Tectonics FP computer program was used to sort the data and to calculate paleostress tensors (Ortner et al. 2002). Only results from those sites are reported where measurements are related to a significant (four and more) number of fault-striae pairs after separation of data.

The number of overprint criteria is limited. However, a detailed analysis allows us to infer a specific succession of brittle

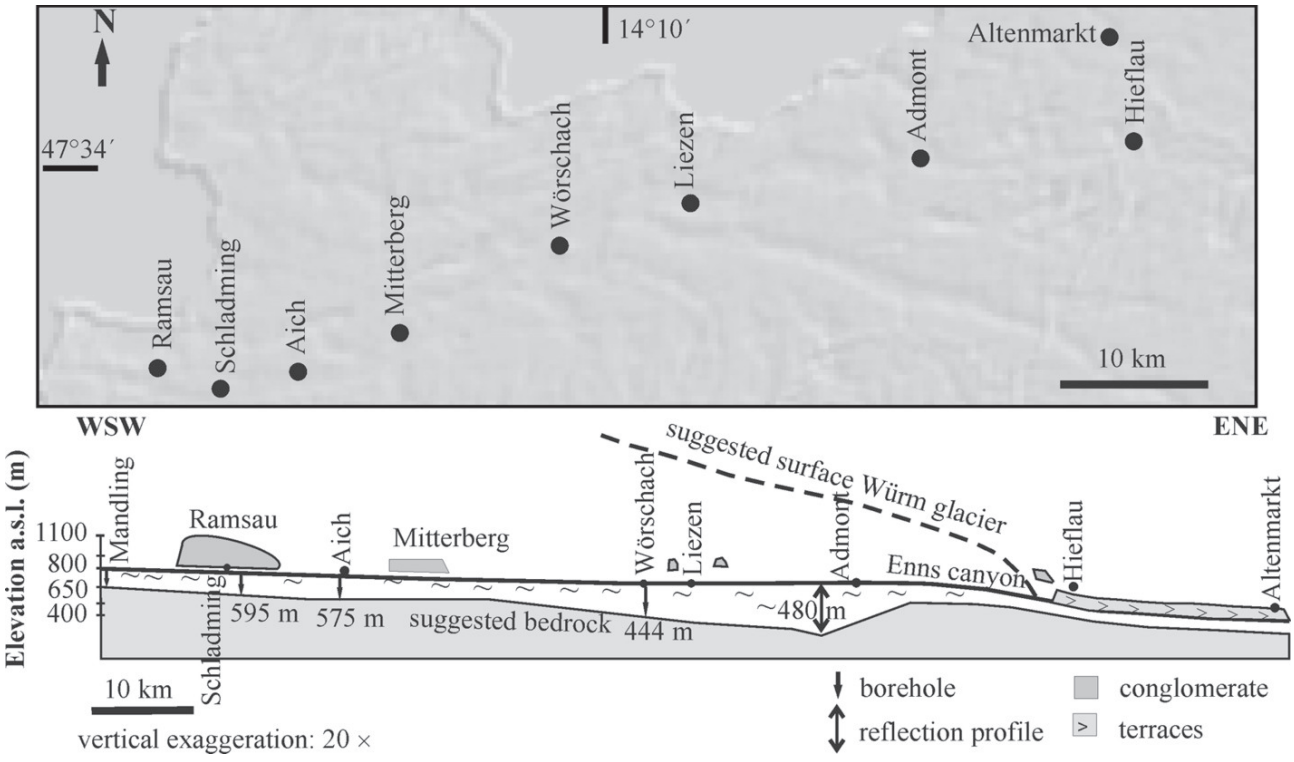

Fig. 8. Geographical setting of locations indicated in a sketch of glacial overdeepening in the Upper Enns Valley from Mandling to Hieflau (modified after Becker 1987 & van Husen 1987; sources of drill hole data STEWEAG 1978).

tectonic events (see below). The same is valid for the timing as no Cenozoic sediments are exposed in the working area, which would allow us to construct a paleostress stratigraphy. For that purpose, we follow the analyses of Peresson & Decker (1997a,b) from the adjacent Northern Calcareous Alps and of Wang & Neubauer (1998) from the SEMP fault west of the study area. The timing given in these studies is based on interferences with the Miocene sedimentary deposits and Oligocene metamorphism in the Tauern Window.

Figures 9 and 10 show the results of the paleostress analysis. We found four distinct paleostress tensor groups labelled A to D.

• Paleostress tensor group A defines an event with N–S compression and mainly strike-slip faults. NW-trending dextral and NNE- to NE-trending sinistral strike-slip faults dominate. S-dipping thrust faults are subordinate. Chlorite and quartz fibers on fault surfaces indicate motion under hydrothermal conditions. Consequently, rocks were at 3–6 km depth beneath the surface during fault motion. The suggested formation time is Late Cretaceous to Paleogene (see Discussion section).

• Paleostress tensor group B comprises E/SE and W/NW-dipping normal faults indicating E–W extension which overprints the former N–S compressional structures (e.g. outcrop no. 15 in Figure 9). This set is also characterized by chlorite- and quartz fibers, again indicating formation under hydrothermal conditions. Furthermore, in two cases, we found N–S extension (labelled paleostress tensor group B_2) on mostly S-dipping normal faults. No overprint criteria were found for this group. The limited number of group B_2 leaves it uninterpretable.

• Paleostress tensor group C comprises ca. N–S trending sinistral strike-slip faults and ca. E–W trending, steeply S-dipping dextral strike-slip faults. Together, these faults indicate ca. NW–SE compression, also indicating a dextral shear along the ENE-trending SEMP fault. Wang & Neubauer (1998) assume a pre-Early Miocene age for this group of faults because it is not recorded in the Miocene Wagrain Basin. Overprints on the older fault sets were observed at localities 3, 6 and 10 (Fig. 9).

• Paleostress tensor group D comprises ca. ENE-trending dextral and NW to NNW-trending sinistral strike-slip faults together constituting ca. E–W compression. Peresson & Decker (1997a,b) assume a Pliocene age for this group.

Interestingly, virtually no record of sinistral shear along the SEMP fault was found.

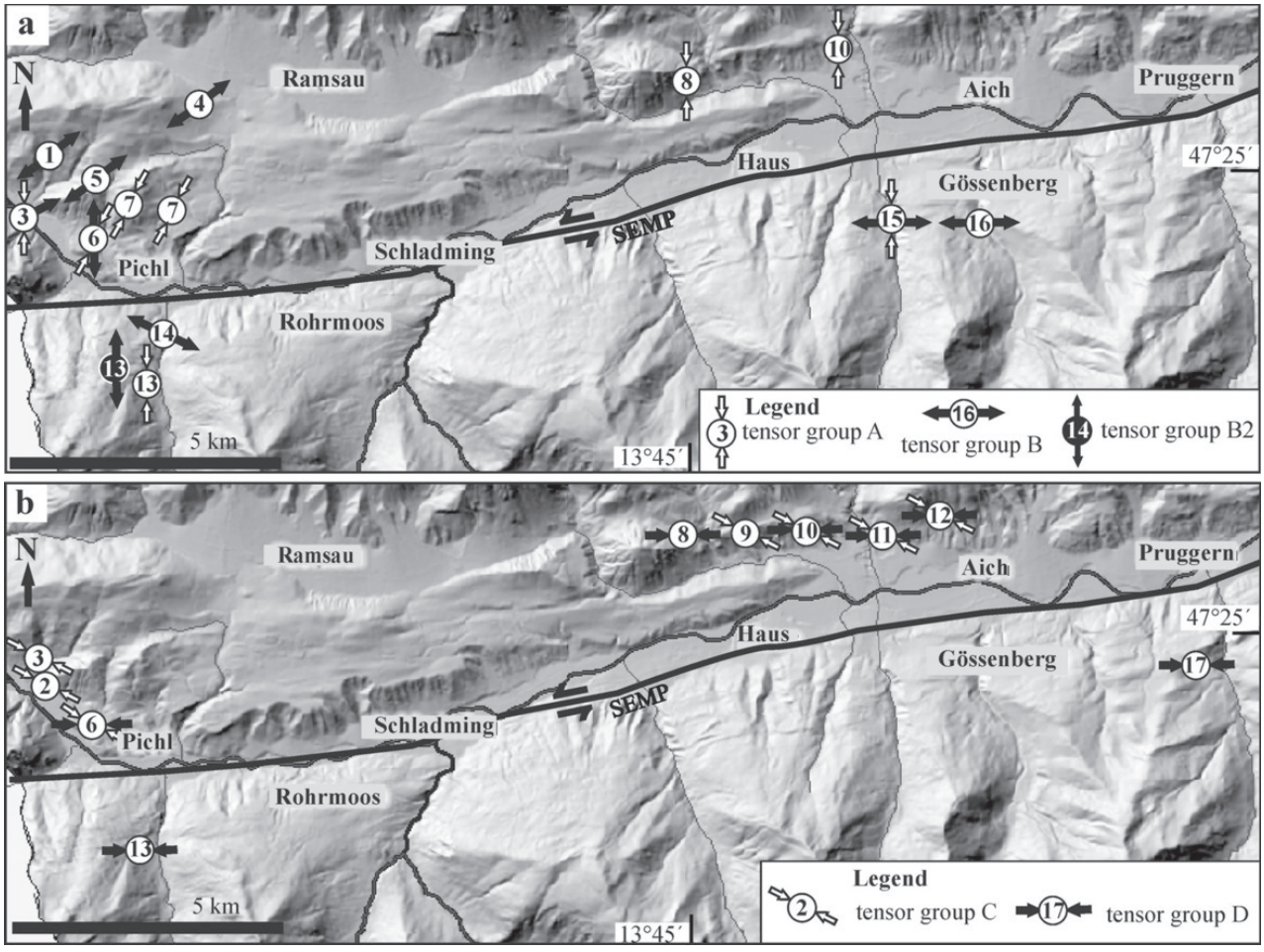

Fig. 9. a — Localities of paleostress tensor groups A and B, **b** — Localities of paleostress tensor groups C and D.

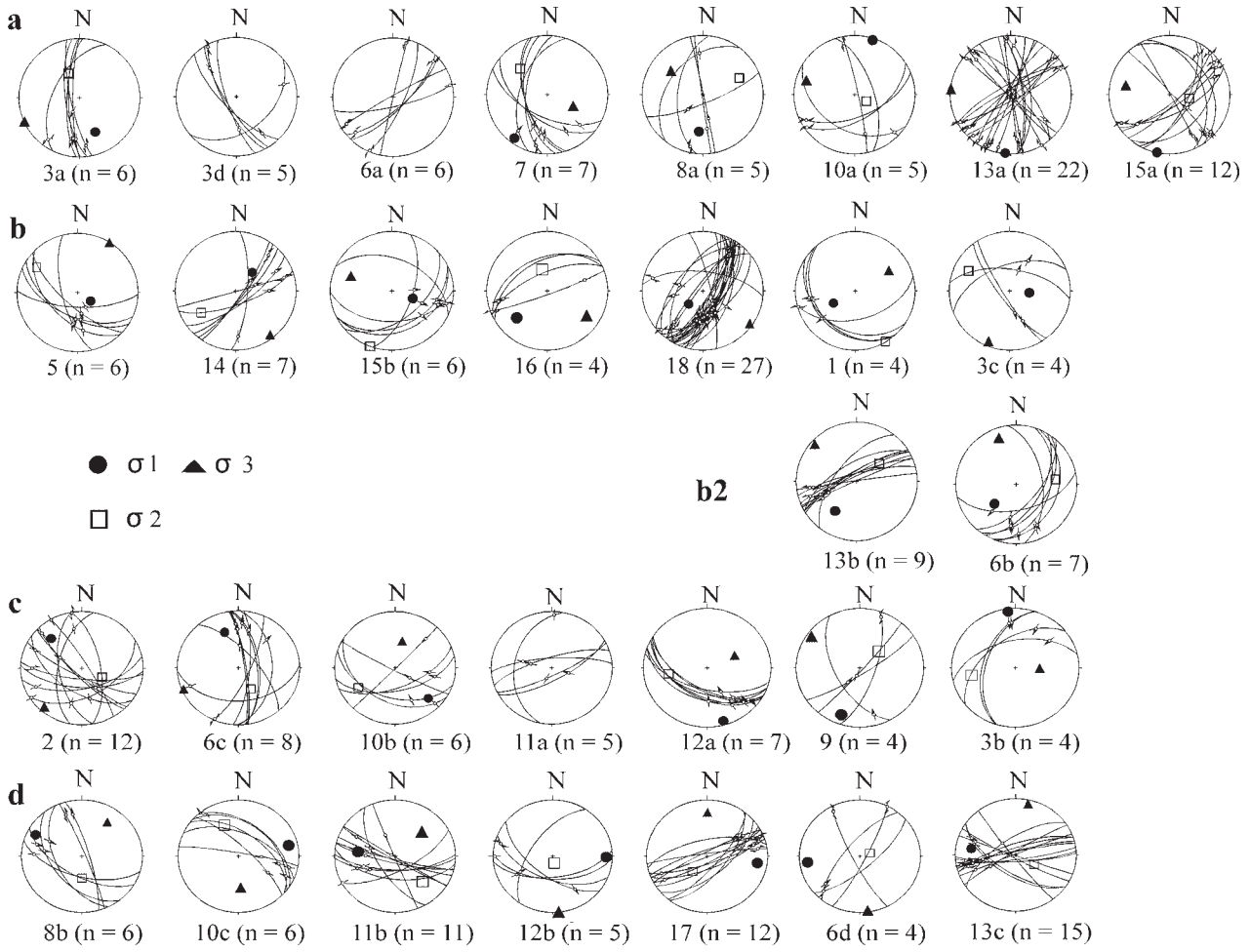

Fig. 10. Fault and striae data and their paleostress assessment from basement rocks along the SEMP and Mandling faults. Numbers according to localities in Fig. 9 and Table 2; lower hemisphere equal-area projections.

Ramsau Conglomerate Formation: deformation structures

Shallow dip of bedding (2–10°) is found in the Ramsau Conglomerate Formation near the edge of the Ramsau plateau (Fig. 11). Bedding planes with dip angles >30° are developed at lower elevations and farther east close to the base of the Ramsau Conglomerate Formation, near Birnberg where normal faults are exposed. The moderately W-dipping bedding planes are associated with listric normal faults; they represent, therefore, rollover-type structures.

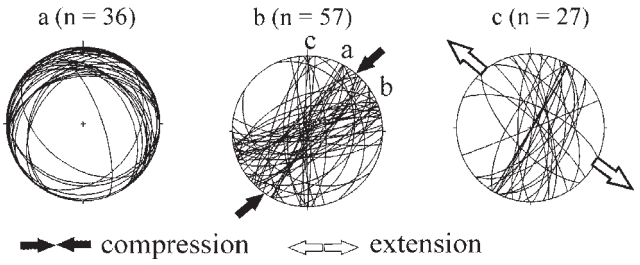

Fig. 11. Ramsau Conglomerate Formation: (**a**) orientation of bedding planes, (**b**) joints and (**c**) faults; lower hemisphere equal-area projection.

In many outcrops joints are steep to subvertical and show three trends: a) ENE, b) NE and c) N. The first two sets can be interpreted as conjugate Mohr fractures (Fig. 11b, sets a, b) and the N–S trending joints as extensional structures (Fig. 11b, set c). The conjugate Mohr fractures indicate ca. NE–SW contraction (as shown in Fig. 11b), the N-trending joints E-extension, roughly consistent with normal faults.

Normal faults in several outcrops coincide in orientation with NNE-dipping joints (Fig. 11c). Particular impressive examples of nearly vertical faults can be found on the road Schladming–Ramsau Leiten (Fig. 12, location L in Figure 3).

The dip of faults is perpendicular to valley slopes excluding an origin as mass movement; they dip steeply, or with medium angle, to the ESE. Primarily, these faults indicate WNW–ESE to E–W extension. We observed regularly orientated offsets of ca. 1.0 to 1.2 m.

A lignite seam is intercalated in the Ramsau Conglomerate Formation at middle stratigraphic levels. The lignite seam is flat-lying and can be traced in a W–E direction for about six kilometers (Weiss 2007). The original underground-mining map indicates several faults ("*Sprung*"). Two orientations are

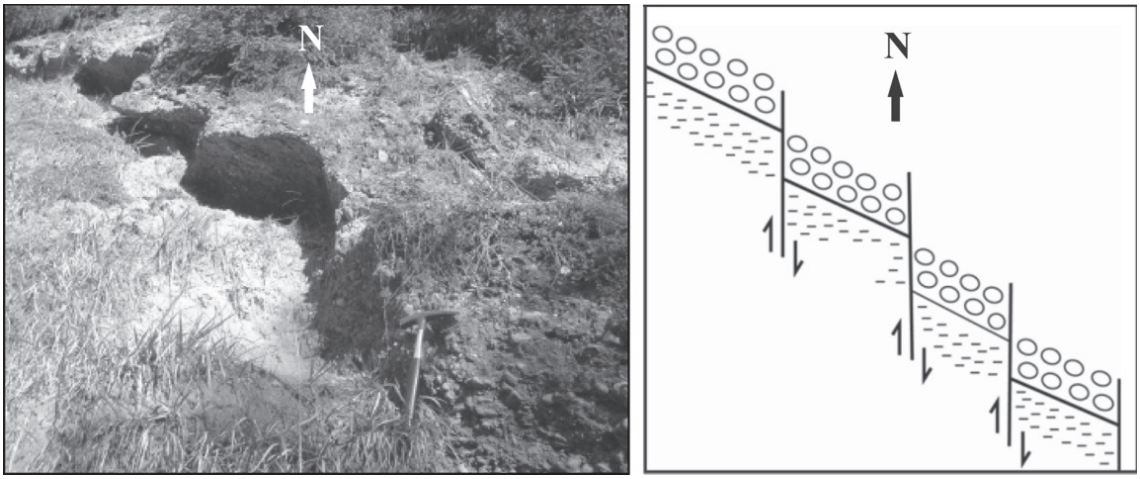

Fig. 12. Field photograph and a parallel scheme showing an array of steep normal faults within the Ramsau Conglomerate Formation, NE Schladming.

reported in the map: ca. E-trending faults with the northern block down, and ca. NNE-trending faults with the eastern block down. Weber & Weiss (1983) report vertical offsets of ca. 2.5 meters at maximum. The NNE-trending normal faults are subparallel to normal faults of surface exposures within the Ramsau Conglomerate Formation.

Photolineaments have been studied from the Ramsau plateau and Mitterberg using digital elevation models (Fig. 13). The Ramsau plateau displays several ca. E- and subordinate NNE-trending lineaments, which can be traced ca. 1.5 to 3 km. Some N- to NNW-trending lineaments are much shorter. The E-trending lineaments of the Ramsau plateau are similar in orientation to the E-trending normal fault of the lignite seam and suggest N–S extension. The N-trending lineaments correspond to the N-trending measured surface structures of the Ramsau Conglomerate Formation.

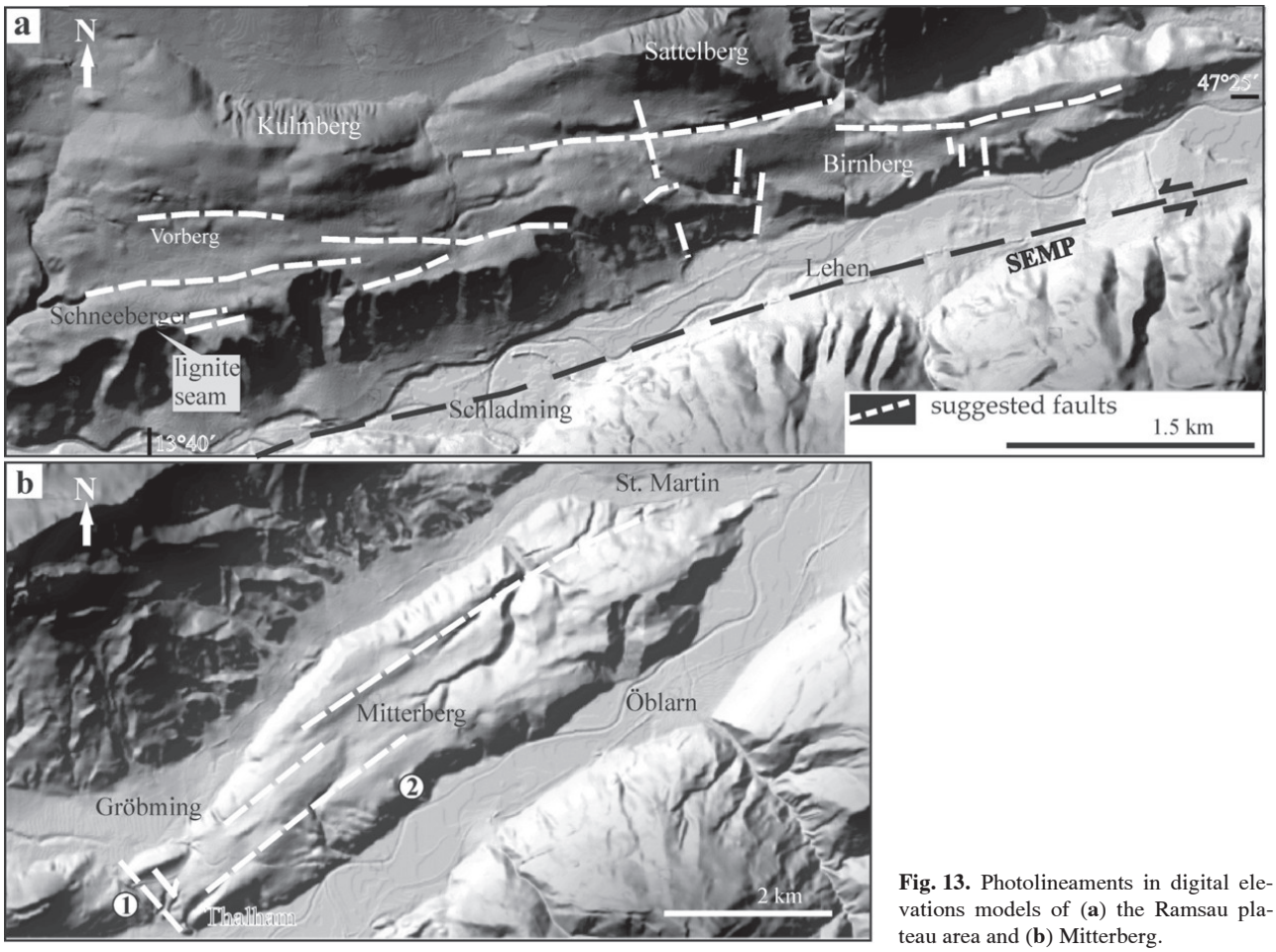

Fig. 13. Photolineaments in digital elevations models of (**a**) the Ramsau plateau area and (**b**) Mitterberg.

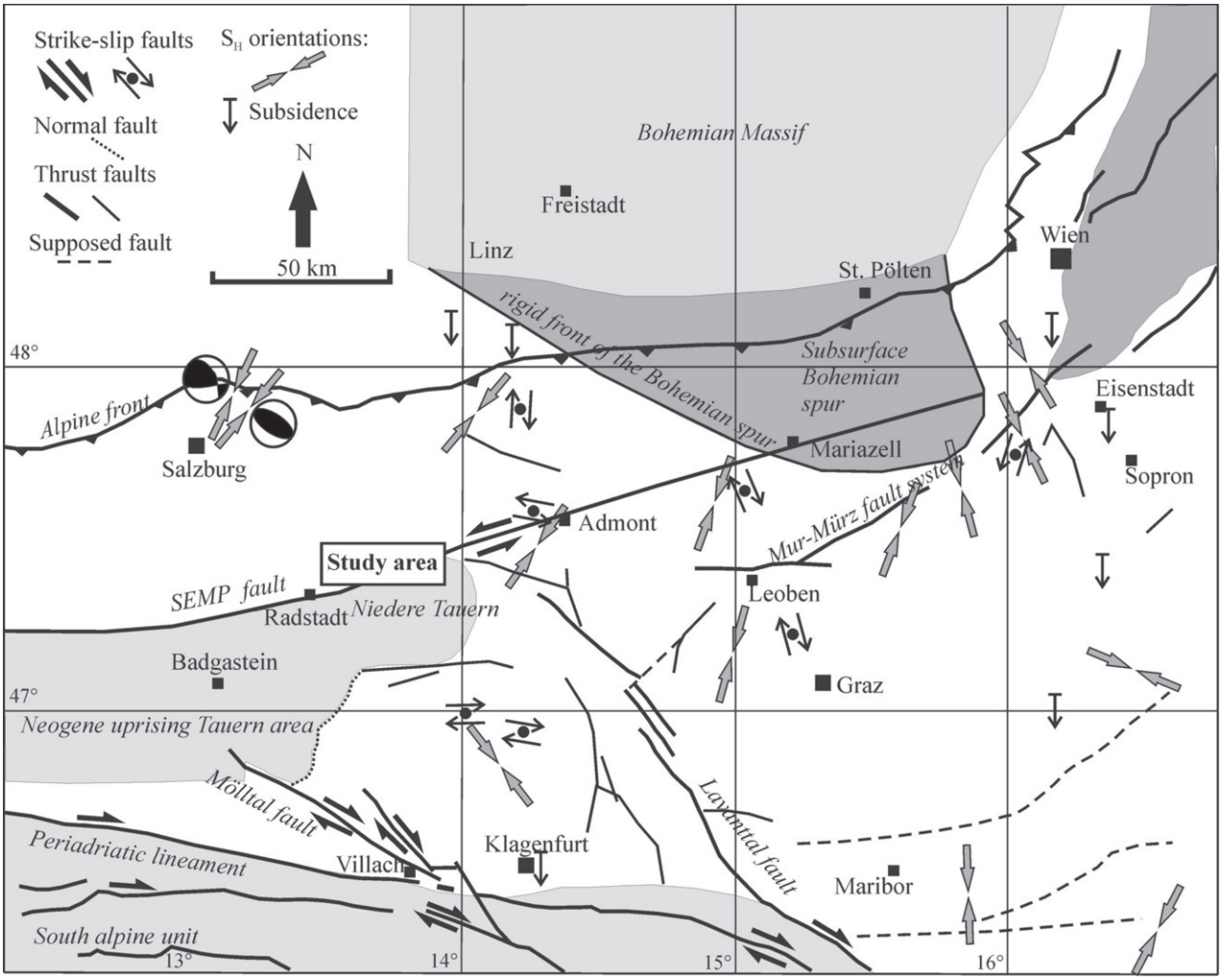

Fig. 14. Stress S_H orientations of the eastern sectors of the Eastern Alps (modified after Reinecker & Lenhardt 1999).

ENE-trending lineaments occur on Mitterberg (Fig. 13b). A further, prominent NW-trending lineament cuts the Mitterberg block in the west; geomorphic evidence argues for a dextral displacement (Fig. 13b, point 1; Table 2, site 17). A NNW-dipping normal fault within the Ramsau Conglomerate Formation was observed at location 2 (Fig. 13b).

In summary, trends of surface joints and faults conform in their orientation and prove similar kinematics as subsurface faults and photolineaments: (1) ca. N–S extension, (2) ca. ESE–WNW to E–W extension, and (3) NE–SW compression, which is recorded only in conjugate Mohr fractures. The development of the latter two could be related to the same stress field.

Recent seismicity

The Upper Enns Valley is not indicated as an area of intense seismicity, but within the polygon grid Ennstal 111 seismic events have been recorded between 1987 and 2005 (Rieder, pers. comm. 2005); magnitudes were between 0.7 and 4.1. These earthquakes were rather shallow; hypocenters are located at a depth between 6 and 8 km (Lenhardt et al. 2007). However, as if to underline our work, an earthquake occurred in the study area on July 19th, 2008 with a magnitude of 3.8 and an epicentral intensity of 5 EMS (European Macroseismic Scale).

Fault plane solutions are only available from adjacent regions (Fig. 14, NNE of Salzburg). The orientation of maximum compression trends either NE–SW or NNE–SSW (Reinecker & Lenhardt 1999; Lenhardt et al. 2007) corresponding to paleostress orientations deduced from fault orientations within the Ramsau Conglomerate Formation (see above).

Discussion

In the following, we discuss the different aspects that contributed to the evolution of the Upper Enns Valley. First, we discuss the paleostress evolution of the SEMP fault in the context of the evolution of the Upper Enns Valley, the development of the drainage pattern, then Quaternary events as recorded by the Ramsau Conglomerate Formation, surface uplift/incision rates, glacial overdeepening and recent seis-

micity. A further description and discussion of vertical motion north and south of the SEMP fault/Upper Enns Valley can be found in Keil & Neubauer (2009).

Kinematics and paleostress evolution

Paleostress tensor orientations of slickensides and striae along the tributaries of the Enns River and apart from the Ramsau Conglomerate Formation record four different stress groups compared to the six stress groups of Peresson & Decker (1997) east of our working area along the SEMP fault. We show below that our data are in part significantly different from those of Peresson & Decker (1997). A partly similar succession of deformation events has been found within and around the Wagrain Basin (Neubauer 2007) and along the SEMP fault at the northern margin of the Tauern Window.

- Paleostress tensor group A indicates N–S strike-slip compression. The event displays abundant evidence for hydrothermal activity resulting in quartz and chlorite fiber growth. Similar events are recorded for deformation related to ductile to brittle low angle normal faults formed in T-conditions of ca. 200–300 °C, leading to the subsidence of Upper Cretaceous to Paleogene Gosau basins (e.g. Neubauer et al. 1995; Koroknai et al. 1999). However, Peresson & Decker (1997a) assume a Late Eocene to questionable Oligocene age in the Northern Calcareous Alps.
- Group B is concentrated in the western section of the Enns Valley. High-angle normal faults with quartz- and chlorite fibers indicate ca. E–W extension, a widespread orientation in Austroalpine units, and possibly suggest the waning stage of the Gosau E–W extension event (e.g. Neubauer et al. 1995; Koroknai et al. 1999). In accordance with their data, we assume therefore, a Late Cretaceous to Paleogene age for paleostress tensor groups A and B. The timing of groups A and B is different to that from Peresson & Decker (1997a), and does not go conform to the topic of the paper.
- Group C (NW–SE compression) occurs along the total length of the study area (12 km) only north of the SEMP fault. We suggest that group C already indicates the onset of reactivation along the sinistral SEMP fault, as at locations 3, 6, 10 in Figure 9.
- Group D recording ca. E–W strike-slip compression indicates the end of the lateral tectonic extrusion event and suggests reactivation by dextral inversion of the initially sinistral SEMP. A similar reactivation has been described by Peresson & Decker (1997a,b) for the eastern part of the SEMP fault and by Hinsch et al. (2005) for the Vienna Basin. These authors assume a Pliocene age for this stage. E–W compression again only affects the northern side of the Upper Enns Valley.
- The most interesting result is that hardly any evidence for sinistral strike-slip and oblique-slip motion along steeply NNW-dipping faults has been found in the working area as could have been expected from the sinistral nature of the SEMP fault as revealed by geological reasons.

A further result is that deformation is not reflected in brittle structures in basement rocks except the scarce evidence for N–S extension in paleostress tensor group B_2.

Evolution of drainage pattern

The drainage pattern of the Eastern Alps largely reflects extrusion tectonics (Frisch et al. 2000a; Robl et al. 2008b) and major rivers like the Enns River follow major faults of the extrusional wedge. The formation of the drainage system is connected with fault activity. Robl et al. (2008a) assume that the elbow-shaped bend of the Enns River near Hieflau is a consequence of displacement along the SEMP. A similar phenomenon characterizes the Enns River SE of Mitterberg, where it turns from E to N. However, the impact of glaciations may be responsible for the reorganization of the drainage system, as well.

The steep slopes on the southern side of the Enns River can be seen as a result of neotectonics, and/or of glacial overdeepening (Székely et al. 2002). Erosion in the tributary courses is enhanced by the high gradients and lithological erodability. Erosion that deepens the river valleys but does not erode peaks reduces the mass of an area and leads to peak uplift as a consequence of isostatic adjustment (Burbank & Anderson 2001). Such a process by glacial overdeepening and widening of valleys was considered to be responsible for Quaternary surface uplift by Pelletier (2008). The high rate of stream incision below the paleosurfaces south of the Enns River could be considered as proportional to shear stress exerted by turbulent flowing conditions of the tributaries (Schlunegger et al. 2001). This possibly explains the profile geometry in a tectonically active area. Surface uplift and incision rates are higher south of the Enns River than north of it. The tributaries from the north show a significantly low stream gradient over long distances. A series of triangular facets borders the abrupt transition to a lower gradient; these facets in connection with the low stream gradient and the distally flowing Enns River could be the result of a slower surface uplift rate at the northern side of the valley. Obviously, tectonic and morphological perturbations are more effective in the southern part of the Upper Enns Valley. Consequently, this leads to the assumption that the SEMP strike-slip fault primarily affects the southern side of the valley.

Relating to Becker (1981, 1987) that the Upper Enns Valley was filled up to ca. 1050 m during the Riss/Würm Interglacial, the correlation of the paleosurfaces at ca. 1000–1100 m and 800–900 m on both sides of the Enns Valley during the Quaternary suggests interglacial valley bottoms. Thus, the river profiles may be used to document surface uplift/incision since the last glaciation (Fig. 5).

Glacial overdeepening

The present-day U-shaped Enns Valley profile is explained by glacial overdeepening. However, the overdeepened longitudinal orogen-parallel Upper Enns Valley follows the tectonic structure of the SEMP fault. Tectonic subsidence can be a reason for overdeepening in addition to the formation by glacial erosion (Reitner & van Husen 2007). The thickness of Alpine valley infill and the depth of the underlying bedrock is being discussed (Brocard et al. 2003). The filling actually depends on the relation of the main river to its tributaries; the Enns Valley glacier was re-

sponsible for a base level lowering of 100–200 m (Robl et al. 2008a). Glacial valley overdeepening caused elevated stream power in the southern tributaries and, consequently led to steepening of the slopes in the Ennstal Quartzphyllite areas south of the Enns River. The base of the Ramsau Conglomerate Formation at 820–780 m a.s.l. can also be interpreted as a previous stage of glacial overdeepening during the Riss glaciation. After deglaciation, deposits filled the valley up to ca. 1100 m a.s.l. and formed the base for re-incision.

Origin of the Ramsau Conglomerate Formation

The composition of the Ramsau Conglomerate Formation demonstrates the great variety of the drainage area of the Upper Enns Valley; an exact inventory directly refers to the source of material, as the different components of the conglomerate are mostly rock fragments (Füchtbauer 1988). Analysis of components from the Ramsau Conglomerate Formation results in a predominant percentage of crystalline clasts at all stratigraphic levels (Fig. 7). Even 90 km farther east petrographic studies show clasts from the Upper Enns Valley with prevailing crystalline origin (Spaun 1964) implying a source from southern tributaries of the Enns River. The specific composition of clasts (61 % crystalline rocks) suggests primarily the provenance from the medium and low-grade metamorphic gneissic terrain of the Niedere Tauern, though transport-resistant components (quartzite, gneiss) prevail in all exposures; material from the Northern Calcareous Alps is subordinate (24 % unmetamorphic carbonates, 15 % sandstone).

Quaternary surface uplift

Several processes induce surface uplift. Erosional denudation results in rather low uplift rates of less than 1 mm/yr (Ruess & Höggerl 2002). Higher uplift rates can be reached by plate motion when shortening is converted into crustal thickening and therefore into isostatic uplift. In this case, the uplift is also lower than horizontal plate motion. Finally, glacial unloading can also result in surface uplift in order of mm/yr in time scales of ca. 10 kyr. In the following, we try to quantify uplift, or river incision for the Upper Enns Valley.

The age of the Ramsau Conglomerate Formation is still uncertain; the embedded lignite seam at an altitude of about 965 m could be a clue for dating the conglomerate. The age of the lignite seam has been dated to 30,700 yr ± 1200 yr by the ^{14}C method (van Husen 1987). The valley floor of the Upper Enns Valley is located at 738 m a.s.l.; the highest outcrops of the conglomerate are around 1100 m a.s.l. The difference in elevation leads to the conclusion of an uplift, or Enns River incision of ca. 360 m. If we assume that there has been an uplift of about 360 m during the last 30 kyr, then this dating results in an unrealistic uplif/incision of 12 mm/yr. The main driving forces of uplift/incision include erosional, glacial or deep-lithospheric unloading, plate motion or a mixture of all these processes (Székely et al. 2002). The Adriatic microplate moves northward at about 2.5 mm/yr (D'Agostino et al. 2005; Grenerczy et al. 2005). If we assume the plate motion as the main driving force, the uplift/incision rate has a maximum 2.5 mm/yr, in spite of the present low convergence rate. If we take into account that deposition of the lignite seam occurred already at the beginning of the last Interglacial at about 120 ka BP as our new ^{14}C-date allows us to assume, then the surface uplift could be explained by tectonic uplift with a minor component of post-glacial unloading (Székely et al. 2002). The average vertical difference between the valley bottom and the Ramsau plateau is ca. 300 m; thus, the result seems very reasonable (300 m/120,000 yr = 2.5 mm/yr). The new minimum value of the lignite indicates an age of > 53.3 ka and strengthens our hypothesis.

Estimate of surface uplift

Paleosurfaces have been identified in several mountain ranges (Burbank & Anderson 2001). Because the paleosurfaces were estimated to be about 120 ka old, subtraction of the present topography from this date might define the mean incision value. We observed that the generally steeper slopes between the flat reaches and the valley bottom on the southern side of the Upper Enns Valley promote high erosion rates. The S–N longitudinal profiles to the Enns Valley bottom indicate an average uplift rate of 2.4 mm/yr and an incision up to ca. 300 m (Fig. 5). Generally, valleys following a fault zone show enhanced incision rates (Robl et al. 2008a). The average uplift rate of the paleosurfaces differs widely from the average surface uplift of the Niedere Tauern (> 1 mm/yr relative to the Bohemian Massif according to Ruess & Höggerl 2002). Paleosurfaces south of the Upper Enns Valley partly display different elevations and do not match exactly with the Ramsau plateau. In our opinion the presence of terraces, or paleosurfaces at different elevations indicate differential uplift on both sides of the Upper Enns Valley. On the one hand, different uplift rates are due to lithological differences between the N and S of the valley, and on the other hand due to the isostatic rebound of the deglaciation (Székely et al. 2002).

Quaternary deformation

The NNE-trending normal faults observed in the former coal mine conform in orientation to joints and faults within the Ramsau Conglomerate Formation and indicate a WNW–ESE orientation of the minimal horizontal stress that suggests WNW–ESE extension. WNW–ESE extension may be correlated with the overall extension during the Miocene lateral extrusion process (Frisch et al. 2001). The lignite seam shows offsets up to 2.5 m, certainly formed later than the lignite (Weber & Weiss 1983). The high-angle normal faults give proof of recent neotectonic activity and are the consequence of ongoing uplift of the Northern Calcareous Alps and lateral extrusion. The lignite seam is likely to have formed during the warm period of the last Pleistocene Interglacial (Draxler 1977). The documented normal faults therefore record a post-Eem Interglacial deformation. A normal fault in the western part of the underground mine records ca. NNW–SSE extension and this event is consistent with the paleostress tensor of the so far uninterpretable group B_2. The WNW–ESE extension of the second fault is consistent with surface observa-

tions and with fault plane solutions of ongoing seismicity (Reinecker & Lenhardt 1999).

WNW–ESE extension in most exposures resulted in tilting of some portions of the Ramsau Conglomerate Formation. The minimum horizontal stress is assumed to have a uniform WNW to ESE orientation. This orientation of recent stress has already been observed within the highest tectonic stratigraphic units, such as the Northern Calcareous Alps (Reinecker & Lenhardt 1999; Neubauer & Genser 1989) and within the Tauern Window (Wang & Neubauer 1998). Active orogen-parallel E-W extension can be observed on the Brenner Normal Fault, on the western border of the Tauern Window, in the Engadine and the Italian Eastern Alps (Reiter et al. 2005).

Recent seismicity

The regional stress field caused by the indentation of the Adria/Southalpine indenter is considered to control local paleostress orientations of the Austroalpine and Penninic units of the Eastern Alps along the western (e.g. Wang & Neubauer 1998) and eastern parts of the SEMP fault (Nemes et al. 1995). Further details are available from the Northern Calcareous Alps (Linzer et al. 1997; Peresson & Decker 1997a,b), the southern Vienna Basin (Hinsch et al. 2005), and only a few data are available from active tectonic structures in the study area. Local heterogeneities and discontinuities in uplift and incision seem to play a major role (Reinecker & Lenhardt 1999) when considering the presence of active tectonic structures in a region, situated along the SEMP fault. Between 1900 and 1998, more than 1600 seismic events have been observed in Austria (Lenhardt et al. 2007) related to some major active fault zones, including the SEMP fault. Observations made during field work showed the instability of the Ramsau Conglomerate Formation and the instability in the channels of the southern tributaries. Landslides are often delimited by fractures in the bedrock; an earthquake may easily trigger spreading of unstable lithologies. Measurements of fractures and faults as well as slickensides fortified the assumption of recent neotectonic effects, or suggest that earthquakes occur on reactivated faults and reflect the regional stress field (Hinsch et al. 2005). The NE–SW shortening deduced from conjugate shear fractures of the Ramsau Conglomerate Formation might represent the surface expression of an earthquake-producing stress field. This is consistent with stresses deduced from fault plane solutions from earthquakes, which also indicate a NE–SW oriented maximum principal stress. These orientations of maximum horizontal shortening also occur in paleostress tensors deduced from slickensides within the basement (see above). The NE–SW orientation is explained by the NW-trending edge of the rigid Bohemian spur.

Conclusions

The Upper Enns Valley covers only a small proportion of the surrounding tectonic units, but it covers the typical features of landforms, like valleys, escarpments, steep slopes and plateaus used to interpret its present-day status. The following conclusions display the neotectonics, drainage pattern and geomorphology of the Upper Enns Valley in a regional context.

(1) The number of observed overprint on faults and striae sets derived from the tributary valleys records a succession of four stress groups, timed from Upper Cretaceous to Pliocene, comprising N–S compression, E–W extension, NW–SE compression and E–W compression. Thus, the present-day topography of the Upper Enns Valley is the result of changing stress fields, of activated or re-activated events along the SEMP fault, underlined by shallow earthquakes occurring in the area. WNW–ESE extension indicated on a mining map is consistent with surface observations in the Ramsau Conglomerate Formation and with fault plane solutions NNE of Salzburg.

(2) The predominant percentage of crystalline clasts in the Ramsau Conglomerate Formation up to the Ramsau plateau at ca. 1100 m and on Mitterberg at ca. 900 m indicates the material supply from the Schladming basement terrain. The Ramsau plateau and the Mitterberg count as relics and formed a continuous Pleistocene valley bottom with the paleosurfaces south of the Upper Enns Valley.

(3) Based upon the Ramsau Conglomerate Formation, the Pleistocene valley bottom is informative to trace back incision and uplift rates. However, dating of the conglomerate is still problematic. The so far published data about the age of the lignite seam (31 ± 1.2 ka) which is intercalated in the Ramsau Conglomerate Formation is disproved. The data do not match with uplift and incision. An older age of the lignite seam seems more realistic. The ^{14}C abundance is below detection limit representing a ^{14}C-age older than 53,300 years. An assumed age of deposition of the lignite ca. 120 ka BP indicates a reasonable uplift/incision rate (2.4–3 mm/yr).

(4) Geomorphic units like steep slopes, high erosion rates and the lithological differences between N and S of the Upper Enns Valley lead to a locally differential uplift history.

Acknowledgments: The manuscript profited substantially from the detailed and constructive reviews of Wolfgang Frisch and an anonymous reviewer. We gratefully acknowledge Wolfgang Lenhardt for submitting earthquake data and fault plane solutions. Acknowledgement is also given to the Österreichische Geologische Gesellschaft.

References

Becker L.P. 1981: Zur Kenntnis der spätglazialen Entwicklung des mittleren Mandlingtales Stmk./Salzbg.). *Mitt. Naturwiss. Verein Steiermark* 11, 31–37.

Becker L.P. 1987: Die quartären Talfüllungen im Raume Schladming. *Geol. Bundesanst.,* Wien 1987 Blatt 127 Schladming, 124–133.

Brocard G.Y., van der Beek P.A., Bourlès D.L., Siame L.L. & Mugnier J.L. 2003: Long-term fluvial incision rates and postglacial river relaxation time in the French Western Alps from ^{10}Be dating of alluvial terraces with assessment of inheritance, soil development and wind ablation effects. *Earth Planet. Sci. Lett.* 209, 197–214.

Burbank D.W. & Anderson R.S. 2001: Tectonic geomorphology. Oxford, 1–252.

D'Agostino N., Cheloni D., Mantenuto S., Selvaggi G., Michelini A. & Zuliani D. 2005: Strain accumulation in the southern Alps (NE Italy) and deformation at the northeastern boundary of Adria observed by CGPS measurements. *Geophys. Res. Lett.* 32 (19): Art. No. L19306 Oct. 14, 2005.

Draxler I. 1977: Pollenanalytische Untersuchungen von Mooren zur spät- und postglazialen Vegetationsgeschichte im Einzugsgebiet der Traun. *Jb. Geol. Bundesanst.,* Wien 120, 131–163.

Draxler I. & van Husen D. 1978: Zur Einstufung innerwürmzeitlicher Sedimente von Ramsau/Schladming und Hohentauern (Steiermark). *Z. Gletscherkunde und Glaziologie* 14, 105–114.

Dunkl I., Kuhlemann J., Reinecker J. & Frisch W. 2005: Cenozoic relief evolution of the eastern Alps — constraints from Apatite fission track age-Provenance of Neogene intramontane sediments. *Austrian J. Earth Sci.* 98, 92–105.

Frisch W., Kuhlemann J., Dunkl I. & Brügel A. 1998: Palinspastic reconstruction and topographic evolution of the Eastern Alps during late Tertiary tectonic extrusion. *Tectonophysics* 297, 1–15.

Frisch W., Székely B., Kuhlemann J. & Dunkl I. 2000a: Geomorphological evolution of the Eastern Alps in response to Miocene tectonics. *Z. Geomorphologie* 44, 1, 103–138.

Frisch W., Dunkl I. & Kuhlemann J. 2000b: Post-collisional orogen-parallel large-scale extension in the Eastern Alps. *Tectonophysics* 327, 239–265.

Frisch W., Kuhlemann J., Dunkl I. & Székely B. 2001: The Dachstein paleosurface and the Augenstein Formation in the Northern Calcareous Alps — a mosaic stone in the geomorphological evolution of the Eastern Alps. *Int. J. Earth Sci*. 90, 500–518.

Frisch W., Kuhlemann J. & Dunkl I. 2002: Dachstein-Altfläche, Augenstein-Formation und Höhlenentwicklung der letzten 35 Millionen Jahrein den zentralen Nördlichen Kalkalpen. *Die Höhle* 53, 1, 1–37.

Füchtbauer H. 1988: Sedimente und Sedimentgesteine. Stuttgart, 1–1141.

Genser H. & Neubauer F. 1989: Low angle normal faults at the eastern margin of the Tauern window (Eastern Alps). *Mitt. Österr. Geol. Gesell*. 81(1988), 233–243.

Grenerczy G., Sella G.F., Stein S. & Kenyeres A. 2005: Tectonic implications of the GPS velocity field in the northern Adriatic region. *Geophys. Res. Lett.* 32, L16311. doi: 10.1029/2005GL022947.

Hejl E. 1997: Cold spots' during the Cenozoic evolution of the Eastern Alps: Thermochronological interpretation of apatite fission-track data. *Tectonophysics* 272, 159–172.

Hinsch R., Decker K. & Wagreich M. 2005: 3-D mapping of segmented active faults in the southern Vienna Basin. *Quat. Sci. Rev*. 24, 321–336.

Keil M. & Neubauer F. 2009: Initiation and development of a fault-controlled, orogen-parallel overdeepened valley: the Upper Enns Valley, Austria. *Austrian J. Earth Sci*. 102/1, 80–90.

Koroknai B., Neubauer F., Genser J. & Topa D. 1999: Metamorphic and tectonic evolution of the Austroalpine units at the western margin of the Gurktal nappe complex, Eastern Alps. *Schweiz. Mineral. Petrogr. Mitt.* 79, 277–295.

Kuhlemann J., Frisch W., Dunkl I. & Székely B. 2001a: Quantifying tectonic versus erosive denudation by the sediment budget: Miocene core complexes of the Alps. *Tectonophysics* 330, 1–23.

Lenhardt W.A., Freudenthaler C., Lippitsch R. & Fiegweil E. 2007: Focal-depth Distribution in the Austrian Eastern Alps based on macroseismic data. *Austrian J. Earth Sci.* 100, 66–79.

Linzer H.G., Moser F., Nemes F., Ratschbacher L. & Sperner B. 1997: Build-up and dismembering of the eastern Northern Calcareous Alps. *Tectonophysics* 272, 97–124.

Mandl G.W. & Matura A. 1987: Geographisch-geologische Übersicht. *Geol. Bundesanst.* Wien 1987, Blatt 127 Schladming, 5–12.

Mandl G.W. & Matura A. 1995: Geologische Karte der Republik Österreich 1:50,000, 127 Schladming. *Geol Bundesanst*. Wien.

Matura A. 1987: Schladminger Kristallinkomplex. *Geol. Bundesanst*. Wien 1987, Blatt 127 Schladming, 13–21.

Nemes F., Pavlik W. & Moser M. 1995: Geologie und Tektonik im Salzatal (Steiermark) — Kinematik und Paläospannungen entlang des Ennstal-Mariazell-Blattverschiebungssystems in den Nördlichen Kalkalpen. *Jb. Geol. Bundesanst.*, Wien 138, 349–367.

Neubauer F. 2007: Formation of an intra-orogenic transtensional basin: the Neogene Wagrain basin in the Eastern Alps. 8th Workshop on Alpine Geological Studies (Davos/Switzerland, October 10–12, 2007) *Abstract Volume*, 54.

Neubauer F. & Genser J. 1989: Architektur und Kinematik der östlichen Zentralalpen — eine Übersicht. *Mitt. Naturwiss. Ver. Steiermark* 120 (METZ-Festschrift), 203–219.

Neubauer F., Dallmeyer R.D., Dunkl I. & Schirnik D. 1995: Late Cretaceous exhumation of the metamorphic Gleinalm dome, Eastern Alps: kinematics, cooling history and sedimentary response in a sinistral wrench corridor. *Tectonophysics* 242, 79–89.

Neubauer F., Fritz H., Genser J., Kurz W., Nemes F., Wallbrecher E., Wang X. & Willingshofer E. 2000: Structural evolution within an extruding wedge: model and application to the Alpine-Pannonian system. In: Lehner F. & Urai J. (Eds.): Aspects of tectonic faulting. (In Honour of Georg Mandl). *Springer*, Berlin–Heidelberg–New York, 141–153.

Ortner H., Reiter F. & Acs P. 2002: Easy handling of tectonic data: the programs Tectonics VP for Mac and Tectonics FP for Windows. *Computer and Geosciences* 28, 1193–1200.

Pelletier J.D. 2008: Glacial erosion and mountain building. *Geology* 36, 591–592.

Peresson H. & Decker K. 1997a: Far-field effects of Late Miocene subduction in the Eastern Carpathians: E-W compression and inversion of structures in the Alpine-Carpathian-Pannonian region. *Tectonics* 16, 38–56.

Peresson H. & Decker K. 1997b: The Tertiary dynamics of the northern Eastern Alps (Austria): changing Paleostress in a collisional plate boundary. *Tectonophysics* 272, 125–157.

Ratschbacher L., Frisch W., Neubauer F., Schmid S.M. & Neugebauer J. 1989: Extension in compressional orogenic belts: the Eastern Alps. *Geology* 17, 404–407.

Ratschbacher L., Frisch W., Linzer G. & Merle O. 1991: Lateral extrusion in the Eastern Alps, part 2: Structural analysis. *Tectonics* 10, 257–271.

Reinecker J. 2000: Stress and deformation: Miocene to present-day tectonics in the Eastern Alps. *Tübinger Geowiss. Arb. Reihe A 55*.

Reinecker J. & Lenhardt W.A. 1999: Present-day stress field and deformation in eastern Austria. *Int. J. Earth Sci.* 88, 532–550.

Reiter F., Lenhardt W.A. & Brandner R. 2005: Indications for activity of the Brenner Normal Fault zone (Tyrol, Austria) from seismological and GPS data. *Austrian J. Earth Sci.* 97, 16–23.

Reitner J.M. & van Husen D. 2007: Overdeepened valleys in the Eastern Alps: Why are they still interesting? *Geophys. Res. Abstr.*, Vol. 9, 03833.

Ritts B.D., Yue Y. & Graham S.A. 2004: Oligocene-Miocene tectonics and sedimentation along the Altyn Tagh Fault, Northern Tibetan Plateau — analysis of the Xorkol, Subei, and Aksay basins. *J. Geology* 112, 207–229.

Robl J., Hergarten St. & Stüwe K. 2008a: Morphological analysis of the drainage system in the Eastern Alps. *Tectonophysics* 460, 263–277.

Robl J., Stüwe K., Hergarten S. & Evans L. 2008b: Extension during continental convergence in the Eastern Alps: The influence of orogen-scale strike-slip faults. *Geology* 36, 963–966. doi: 10.1130/G25294A.1

Ruess D. & Höggerl N. 2002: Bestimmung rezenter Höhen und

Schwereänderungen in Österreich. *Pangeo Austria 2002,* Programm und Kurzfassungen. University of Salzburg, 1–151.

Sachsenhofer R.F. 1988: Zur Inkohlung des Ennstaltertiärs. *Sitz.-Ber. Österr. Akad. Wiss., Math.-naturwiss. Kl. Abt.* I 197, 333–342.

Sachsenhofer R.F. 2001: Syn- and post-collisional heat flow in the Cenozoic Eastern Alps. *Int. J. Earth Sci.* 90, 579–592.

Schäfer A. 2005: Klastische Sedimente — Fazies und Sequenzstratigraphie. München, 1–414.

Scheidleder A., Boroviczeny F., Graf W., Hofmann Th., Mandl G.W., Schubert G., Stichler W., Trimborn P. & Kralik M. 2001: Pilotprojekt "Karstwasser Dachstein". Band 2: Karsthydrologie und Kontaminationsrisiko von Quellen. *Archiv Lagerstättenforsch. Geol. Bundesanst.* 21, 1–155.

Schlunegger F., Melzer J. & Tucker G.E. 2001: Climate, exposed source-rock lithologies, crustal uplift and surface erosion: a theoretical analysis calibrated with data from the Alps/North Alpine Foreland basin system. *Int. J. Earth Sci*. 90, 484–499.

Schmid Chr., Suette G. & Weber F. 2005: Erste Ergebnisse reflexionsseismischer Messungen im Ennstal zwischen Liezen und Weng (Steiermark). *Jb. Geol. Bundesanst.,* Wien 145, 107–114.

Seebacher R. 2006: Aktuelle Forschungen in der Südwand–Dachsteinloch, 1543/28, Stmk./OÖ. *Die Höhle* 57/1, 76–89.

Spaun G. 1964: Das Quartär im Ennstal zwischen Hieflau und Altenmarkt. *Mitt. Gesell. Geol. Bergbaustud. Wien* 14, 149–184.

Székely B., Reinecker J., Dunkl I., Frisch W. & Kuhlemann J. 2002: Neotectonic movements and their geomorphic response as reflected in surface parameters and stress patterns in the Eastern Alps. *EGU Stephan Müller Spec. Publ. Ser.* 3, 149–166.

TRANSALP Working Group: Gebrande H., Lüschen E., Bopp M., Bleibinhaus F., Lammerer B., Oncken O., Stiller M., Kummerow J., Kind R., Millahn K., Grassl H., Neubauer F., Bertelli L., Borrini D., Fantoni R., Pessina C., Sella M., Castellarin A., Nicolich R., Mazzotti A. & Bernabini M. 2002: First deep seismic reflection images of the Eastern Alps reveal giant crustal wedges and transcrustal ramps. *Geophys. Res. Lett.* 29/10, 92–1, 92–4.

van Husen D. 1981: Geologisch-sedimentologische Aspekte im Quartär von Österreich. *Mitt. Österr. Geol. Gesell.* 74/75, 197–230.

van Husen D. 1987: Zur Entwicklung des oberen Ennstales im Pleistozen. *Geol. Bundesanst.* Wien 1987 Blatt 127 Schladming, 86–93.

van Husen D. 2000: Geological processes during the Quaternary. *Mitt. Österr. Geol. Gesell.* 92, 135–156.

Wang X. & Neubauer F. 1998: Orogen-parallel strike-slip faults bordering metamorphic core complexes: the Salzach-Enns fault zone in the Eastern Alps, Austria. *J. Struct. Geol.* 20, 799–818.

Weber L. & Weiss A. 1983: Bergbaugeschichte und Geologie der österreichischen Braunkohlenvorkommen. *Archiv Lagerstättenforschung Geol. Bundesanst*., Wien 4, 1–317.

Weiss A. 2007: Zur Geschichte des Kohlenbergbaus bei Schladming. *Kulturzeitschrift Österr. Mitt.* 28, 6–10.

Yue Y., Bradley D.R., Graham St.A., Wooden G. & Zhang Z. 2003: Slowing extrusion tectonics: lowered estimate of post-Early Miocene slip rate for the Altyn Tagh fault. *Earth Planet. Sci. Lett.* 217, 111–122.

Zentralanstalt für Meteorologie und Geodynamik, Wien 2005: Lenhardt W.A. pers. comm.; Regionalstelle Steiermark 2005: Rieder H. pers. comm.

Zötl J. 1960: Der politische Bezirk Liezen als Landschaft und Lebensraum. Graz, 1–112.

Appendix

Table 1: Results of radiocarbon dating of lignite from the Ramsau Conglomerate Formation.

Laboratory no.	Sample	$\delta^{13}C^{1,2)}$ [‰]	^{14}C-age [BP]
VERA-5152	Ramsau 1	–30.4±1.7	>53,300

[1)] 1σ — error
[2)] $\delta^{13}C$-ratio determined by accelerator mass spectrometry

Table 2: Paleostress in the basement: Geographical setting, GPS coordinates when available, lithology and paleostress tensors. NDA — numerical dynamical analysis, PT — pressure-tension method, R — stress ratio. Locations are shown in Fig. 9.

Site	Coordinates	Set	Geographic setting	Lithology resp. Formation (GWZ — Greywacke Zone; NCA— Northern Calcareous Alps)	Paleostress tensor group	Method	σ1	σ 2	σ 3	R
1			150 m NW of Irxner	GWZ, phyllite	B	NDA	241/56	149/01	059/34	0.39
2			SE of Mandling	NCA, Ramsau Dolomite	C	NDA	316/28	116/60	222/09	0.57
3	N 47°23.460 E 13°35.869	**a**	B 320, Gleiming	GWZ, chlorite-schist, phyllite	A	NDA	156/37	336/53	246/06	0.50
		b	B 320, Gleiming	GWZ, chlorite-schist, phyllite	C	NDA	353/05	260/61	091/58	0.58
		c	B 320, Gleiming	GWZ, chlorite-schist, phyllite	B	NDA	095/63	296/25	202/08	0.48
		d	B 320, Audörfl	GWZ, chlorite-schist, phyllite	A	PT	148/10	227/71	052/26	
4	N 47°24.986 E 13°36.907		Glutserberg Märchenweg	GWZ, phyllite	B	PT	291/36	190/15	081/50	
5	N 47°24.046 E 13°35.874		Grubbach trench right	NCA, light dolomite	B	NDA	124/69	302/21	032/01	0.46
6		**a**	Grubbach	NCA, Ramsau Dolomite	A	PT	008/27	153/64	267/15	
		b	Grubbach	NCA, Ramsau Dolomite	B2	NDA	210/57	075/25	297/18	0.48
		c	Grubbach	NCA, Wetterstein Dolomite	C	NDA	340/34	152/55	247/04	0.58
		d	Grubbach	NCA, Ramsau Dolomite	D	NDA	263/14	071/76	172/03	0.41
7	N 47°24.196 E 13°36.184		Grubbach, left trench	NCA, Ramsau Dolomite	A	NDA	217/10	314/37	114/51	0.54
8	N 47°25.806 E 13°45.071	**a**	Road to Luser waterfall	NCA, light dolomite	A	NDA	270/14	166/43	014/43	0.41
		b	Road to Luser waterfall	NCA, light dolomite	D	NDA	183/26	077/29	307/49	0.58
9	N 47°25.800 E 13°45.948		SE Burgstaller	NCA, Werfen Formation	C	NDA	131/38	348/50	232/22	0.30
10	N 47°26.164 E 13°47.252	**a**	Gradenbach right	NCA, light dolomite	A	NDA	196/04	100/61	288/29	0.51
		b	Gradenbach right	NCA, light dolomite	C	NDA	135/24	240/31	014/50	0.67
		c	Gradenbach right	NCA, light dolomite	D	PT	077/16	338/40	176/43	
11	N 47°26.051 E 13°47.268	**a**	Gradenbach parking	NCA, Guttenstein Limestone	C	PT	133/40	065/15	343/46	
		b	Gradenbach parking	NCA, Guttenstein Limestone	D	PT	264/03	340/68	174/37	
12	N 47°26.080 E 13°47.646	**a**	Aichberg	NCA, Guttenstein Limestone	C	NDA	164/08	260/39	065/50	0.50
		b	Aichberg	NCA, Guttenstein Limestone	D	PT	091/11	168/80	174/00	
13	N 47°22.813 E 13°36.848	**a**	Preunegg	Ennstal Phyllite	A	NDA	185/01	047/89	275/01	0.59
	N 47°22.641 E 13°37.251	**b**	Preunegg SE Pointner	Ennstal Phyllite	B2	NDA	216/39	051/50	312/08	0.51
		c	Preunegg SE Pointner	Ennstal Phyllite	D	NDA	279/27	118/62	013/08	0.45
14			Preunegg "Klamm"	Ennstal Phyllite	B	NDA	041/56	237/33	142/07	0.57
15	N 47°24.393 E 13°47.739		Gumpenbach	Ennstal Phyllite, greenschist	A	NDA	023/20	161/64	287/16	0.52
		a	Gumpenbach	Ennstal Phyllite, greenschist		NDA	162/26	029/54	264/23	0.46
		b	Gumpenbach	Ennstal Phyllite, greenschist	B	NDA	111/60	201/00	291/30	0.45
16			Seewigtal Teufelsschlucht	Ennstal Phyllite, quartzite-chlorite	B	PT	228/33	347/59	123/24	
17	N 47°24.692 E 13°52.795		Sattental	Ennstal Phyllite, chlorite-phyllite	D	NDA	098/17	221/60	001/23	0.41
18			S Mitterberg, between Gröbming and Moosheim	GWZ, chlorite-schist	B	NDA	226/64	033/26	125/05	0.51